PHYSICAL REVIEW E VOLUME 54, NUMBER 4 OCTOBER 1996

Different types of chaos synchronization in two coupled piecewise linear maps

Yuri Maistrenko
Institute of Mathematics, Academy of Sciences of Ukraine, 3 Tereshchenkivska st, Kiev 252601, Ukraine

Tomasz Kapitaniak
Division of Dynamics, Technical University of Lodz, Stefanowskiego 1/15, 90-924 Lodz, Poland

(Received 25 April 1996)

Dynamics of a four-parameter family of two-dimensional piecewise linear endomorphisms which consist of two linearly coupled one-dimensional maps is considered. We show that under analytically given conditions chaotic behavior in both maps can be synchronized. Depending on the coupling the parameters chaotic attractor's synchronized state is characterized by different types of stability. [S1063-651X(96)11409-4]

PACS number(s): 05.45.+b

I. INTRODUCTION

Recently it has been shown that two identical chaotic systems $x'=f(x)$ and $y'=f(y)$ or $x_{n+1}=f(x_n)$ and $y_{n+1}=f(y_n)$ can synchronize, i.e., $|x(t)-y(t)|\to 0$ as $t\to\infty$ or $|x_n-y_n|\to 0$ as $n\to\infty$ [1–10]. Such synchronization has potential practical applications in secure communication [11–13].

Consider the two-dimensional system

$$x_{n+1}=f_{l,p}(x_n)+d_1(y_n-x_n),$$

$$y_{n+1}=f_{l,p}(y_n)+d_1(x_n-y_n) \tag{1}$$

consisting of two linearly coupled identical one-dimensional subsystems governed by

$$x_{n+1}=f_{l,p}(x_n),$$

$$y_{n+1}=f_{l,p}(y_n), \tag{2}$$

where $x,y\in\mathbb{R}$, l and p are systems parameters, $d_{1,2}$ coupling parameters, $l,p,d_{1,2}\in\mathbb{R}$. Assume that $x_{n+1}=f(x_n)$ and $y_{n+1}=f(y_n)$ have a one-dimensional chaotic attractor A.

In the synchronized regime the dynamics of system (1) is restricted to one-dimensional invariant subspace $x_n=y_n$, so the problem of synchronization of chaotic systems can be understood as a problem of stability of one-dimensional chaotic attractor A in two-dimensional phase space [15,16]. Let A be a chaotic attractor. The basin of attraction $\beta(A)$ is the set of points whose ω-limit set is contained in A. In Milnor's definition [14] of an attractor the basin of attraction need not include the whole neighborhood of the attractor, i.e., we can say that A is a Milnor attractor if $\beta(A)$ has a positive Lebesgue measure. For example, a riddled basin [15–18] which has recently been found in practical physical systems [19,20], has a positive Lebesgue measure but does not contain any neighborhood of the attractor. In this case an attractor A is transversely stable in the invariant subspace $x_n=y_n$, but its basin of attraction $\beta(A)$ may be a fat fractal so that any neighborhood of the attractor intersects the basin with a positive measure, but may also intersect the basin of another attractor, with a positive measure. Attractor A is an asymptotically stable attractor if it is Lyapunov stable and $\beta(A)$ contains the neighborhood of A.

In this paper we consider the dynamics of a four-parameter family of two-dimensional piecewise linear endomorphism

$$x_{n+1}=px_n+\frac{l-p}{2}\left(\left|x_n+\frac{1}{l}\right|-\left|x_n-\frac{1}{l}\right|\right)+d_1(y_n-x_n),$$

$$y_{n+1}=py_n+\frac{l-p}{2}\left(\left|y_n+\frac{1}{l}\right|-\left|y_n-\frac{1}{l}\right|\right)+d_2(x_n-y_n), \tag{3}$$

which consists of two linearly coupled one-dimensional maps being a generalization of a skew tent map. Chaotic attractors of a skew tent map have been considered in [21–24,28].

Dynamics of two coupled maps have been investigated in several papers, for example, [25–27]. A system of two coupled tent maps has been investigated by Pikovsky and Grassberger [25]. They found that even when a system has a stable synchronized state, the basin of attraction can be densely filled with periodic points so the attractor is not asymptotically stable. The dynamics of several endomorphisms of the plane constructed by coupling of two logistic maps was considered by Gardini *et al.* [26]. They used the concept of critical curves to determine global bifurcation. Critical curves were used by Celka [27] to estimate synchronization regions of two unidirectionally coupled triangular maps.

The outline of this paper is as follows. Section II recalls some fundamental properties of the one-dimensional map $x_{n+1}=f_{l,p}(x_n)$ considered. In Sec. III we describe general properties of the two-dimensional map (3). We give analytical conditions under which chaotic behavior in both maps can be synchronized. Some particular examples are discussed in Sec. IV where we additionally show that, depending on the coupling parameters, the synchronized state is characterized by different types of stability. Finally, we summarize our results in Sec. V.

II. ONE-DIMENSIONAL MAP

Let $f=f_{l,p}:\mathbb{R}\to\mathbb{R}$ be a one-dimensional map of real line into itself in the form

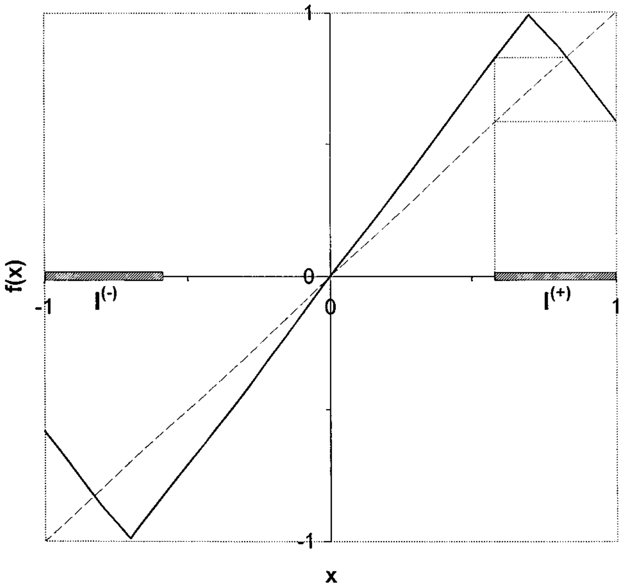

FIG. 1. Graph of the function $f_{l,p}(x)$; $l=-p=\sqrt{2}$.

$$f_{l,p}:x\to px+\frac{(l-p)}{2}\left(\left|x+\frac{1}{l}\right|-\left|x-\frac{1}{l}\right|\right), \qquad (4)$$

where parameters l and p are the slopes. A graph of $f_{l,p}(x)$ is shown in Fig. 1. When

$$(l,p)\in\sum=\left\{l>1,-\frac{2l}{l-1}<p\leqslant-1\right\}$$

$f_{l,p}$ maps interval $[-1,1]$ into itself. If

$$(l,p)\in\prod=\left\{l>1,-\frac{2l}{l-1}<p\leqslant-\frac{l}{l-1}\right\}$$

the whole interval $[-1,1]$ is the chaotic attractor which will be denoted by Γ. Otherwise, i.e., when

$$(l,p)\in\sum_0=\sum\backslash\prod,$$

$f_{l,p}$ has two symmetrical chaotic attractors $I^{(+)}$ and $I^{(-)}$ in the intervals $I^{(+)}=[1+p(l-1)/l,1]$ and $I^{(-)}=[-1,-1-p(l-1)/l]$. In this case map $f_{l,p}$ can be considered as a generalization of the skew tent map investigated in [21–24,28].

Depending on parameters l and p each of these attractors is a cycle of 2^m chaotic intervals $I^{(\pm)}=I_m^{(\pm)}$, $m=0,1,2,\ldots$. Later we will omit the symbol $\pm$ so that it does not cause misunderstanding. Formulas for the parameter region $(l,p)\in\Pi_m$ of the existence of attractors Γ_m can be found in [21–24]. Merging bifurcation $\Gamma_{m+1}\to\Gamma_m$ is caused by the appearance of a trajectory homoclinic to the point cycle γ_m of the period 2^m. In Fig. 1 the function $f_{l,p}$ is plotted in the case $l=-p=\sqrt{2}$ when the bifurcation $\Gamma_1\to\Gamma_0$ takes place.

For any $(l,p)\in\Sigma$ the map $f_{l,p}$ has in the interval $[-1,1]$ a ''good'' invariant measure denoted by $\mu=\mu_{l,p}$ which is absolutely continuous with respect to the Lebesgue measure, with a support $\Gamma_m^{(+)}\cup\Gamma_m^{(-)}$. Let $\rho(x)$ be a probability density function, i.e.,

$$\mu_{l,p}(J)=\int_J\rho(x)dx$$

for any measurable set J $[-1,1]$.

At the bifurcation points $\Gamma_{m+1}\to\Gamma_m$ given by the relation

$$p^{\delta_{m+1}}l^{\delta_m}+(-1)^m(p-1)=0,\quad m=0,1,\ldots$$

where δ_m are obtained from the recurrent relation

$$\delta_{m+1}=2\,\delta_m+\tfrac{1}{2}[1+(-1)^m],\quad m=0,1,\ldots$$

and $\delta_0=1$, probability density function is constant at any component of Γ_{m+1}, hence its values are inversely proportional to the length of the component (the measure of each component of Γ_{m+1} is equal to $2^{(m+1)}$).

Consider the bifurcation $\Gamma_1\to\Gamma_0$ which takes place at $l=p/(1-p^2)$. In this case the fixed point has coordinate $x_1^{(+)}=(p-l)/l(p-1)$, and it can easily be shown that

$$\mu\left(\left[1+\frac{p(l-1)}{l},\ \frac{p-1}{l(p-1)}\right]\right)=\mu\left(\left[\frac{p-l}{l(p-1)},1\right]\right)=\frac{1}{2}$$

and

$$\mu\left(\left[1+\frac{p(l-1)}{l},\ \frac{1}{l}\right]\right)=\frac{p^2-1}{2p^2},$$

$$\mu\left(\left[\frac{1}{l},1\right]\right)=\frac{p^2+1}{2p^2},$$

$$\frac{\mu\left(\left[\frac{1}{l},1\right]\right)}{\mu\left(\left[1+\frac{p(l-1)}{l},\ \frac{1}{l}\right]\right)}=\frac{p^2+1}{p^2-1}.$$

III. TWO-DIMENSIONAL MAP: DIFFERENT TYPES OF THE STABILITY OF SYNCHRONIZED CHAOTIC REGIMES

Let us consider a two-dimensional endomorphism $F=F_{l,p}$ (continuous noninvertable map) of the plane into itself, of the form

$$F_{l,p}:\begin{pmatrix}y\\x\end{pmatrix}\to\begin{pmatrix}f_{l,p}(x)+d_1(x-y)\\f_{l,p}(y)+d_2(y-x)\end{pmatrix},$$

where $f_{l,p}$ has been defined in Sec. I and $d_{1,2}\in\mathbb{R}^l$ are coupling parameters. When $d_{1,2}=0$ mappings along x and y axes are independent. Such a type of an uncoupled map will be denoted by $F_{l,p}^{(0)}$, i.e.,

$$F_{l,p}^{(0)}:\begin{pmatrix}x\\y\end{pmatrix}\to\begin{pmatrix}f_{l,p}(x)\\f_{l,p}(y)\end{pmatrix}.$$

Let $(l,p)\in\Sigma$, then $F_{l,p}^{(0)}$ has an invariant square $I\times I$, where $I=[-1,1]$. If additionally $(l,p)\in\Pi$, this whole square is a

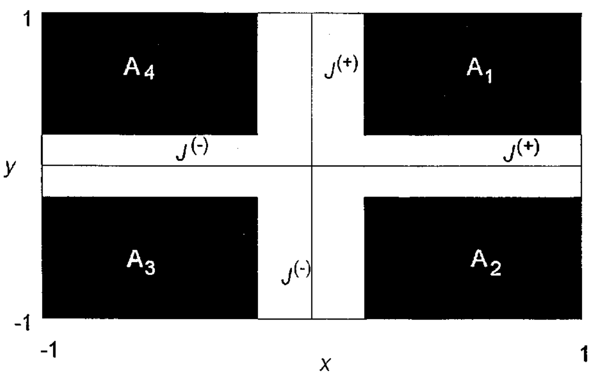

FIG. 2. Attractors of the map $F^{(0)}_{l,p}$, $(l,p)\in\Pi_0\times\Pi_0$.

chaotic attractor. Let $(l,p)\in\Pi_0$, than $F^{(0)}_{l,p}$ has four symmetrical chaotic attractors $A^{(i)}$, $i=1,4$ inside $I\times I$ shown in Fig. 2.

If $(l,p)\in\Pi_m$, $F^{(0)}_{l,p}$ has 4×2^m symmetric chaotic attractors being cycles of chaotic squares of the period 2^m (the so-called period 2^m chaotic attractors).

As the computers experiment presented in Figs. 3(a)–3(d) shows, such types of attractors are preserved at small coupling $|d_{1,2}|\ll 1$—Fig. 3(a), but they disappear when coupling increases—Figures 3(b)–3(d). First attractors far from the main diagonal $x=y$, i.e., $A^{(2)}$ and $A^{(4)}$ are destroyed—Fig. 3(b). Next the survived attractors $A^{(1)}$ and $A^{(3)}$ merge together—Fig. 3(c). In Fig. 3(d) we observe that $x=y$, i.e., chaotic trajectories of x and y subsystems are synchronized and two-dimensional attractors of $F_{l,p}$ are reduced to the two symmetrical one-dimensional attractors at the main diagonal $x=y$. It should be mentioned that the main diagonal $x=y$ is invariant with respect to $F_{l,p}$ for any $d_{1,2}$, and the mapping along it coincides with $f_{l,p}$. As a result $F_{l,p}$ has one eigendirection $\mathbf{u}_1=(1,1)$ which is parallel to the main diagonal, its multiplicator coincides with the multiplicator of $f_{l,p}$

$$\nu_1=\begin{cases} l, & |x|<\dfrac{1}{l}, \\ p, & |x|>\dfrac{1}{l}, \end{cases}$$

and, therefore, the first Lyapunov exponent λ_1 is always positive.

The second eigendirection $\mathbf{u}_2=(d_1,-d_2)$ (exists if $|d_1|+|d_2|\neq 0$) is also invariant for any point of the main diagonal. Its multiplicator is also given in an explicit form

$$\nu_2=\begin{cases} l-(d_1+d_2) & |x|<\dfrac{1}{l} \\ p-(d_1+d_2) & |x|>\dfrac{l}{l}. \end{cases} \tag{5}$$

The property of parallelness of the second eigendirection for any point of the main diagonal allows us to obtain the condition for stability of the chaotic attractor at the main diagonal, which can be written as

$$|l-(d_1+d_2)||p-(d_1+d_2)|^{(\mu/1-\mu)}<1, \tag{6}$$

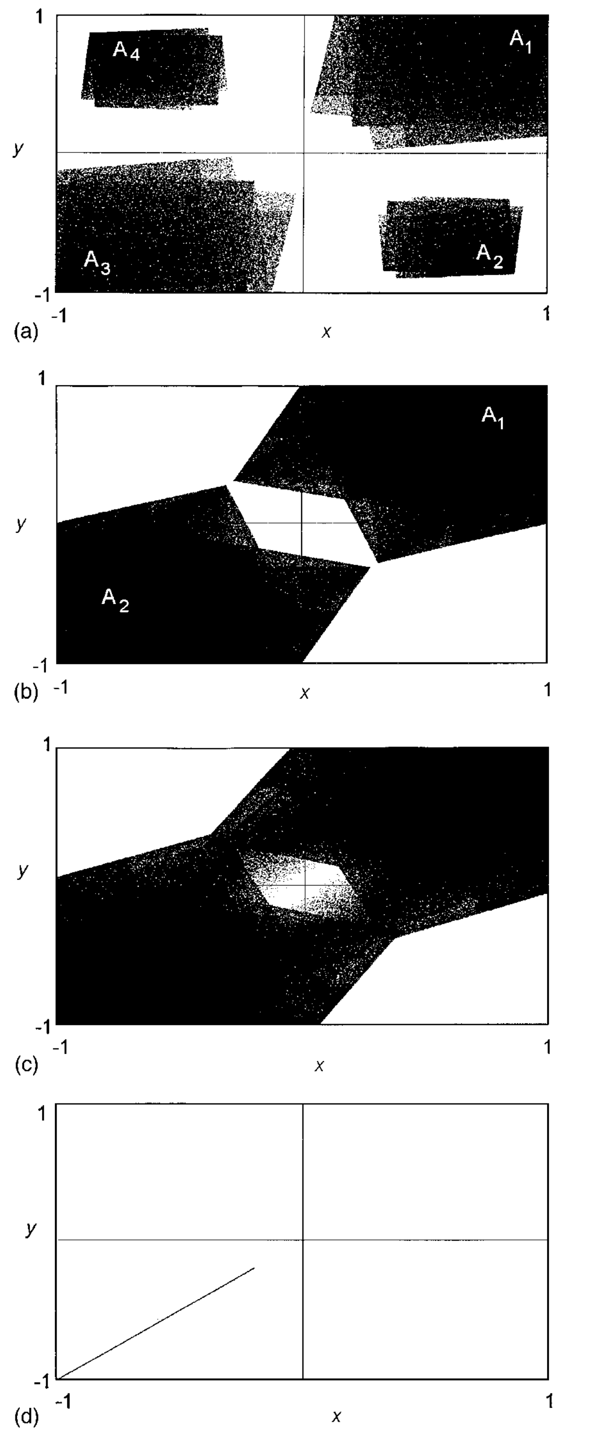

FIG. 3. Attractors of the map $F_{l,p}$; $l=1.5$, $p=-2.4$; (a) $d_1=d_2=0.1$, (b) $d_1=d_2=0.25$, (c) $d_1=d_2=0.3$, (d) $d_1=d_2=0.6$.

where $\mu=\mu_{l,p}(\{|x|\geq 1/l\})$. One can easily check that it is a condition of negativeness of the second Lyapunov exponent of the attractor.

$$\lambda_2=(1-\mu)\ln|l-(d_1+d_2)|+\mu\ \ln|p-(d_1+d_2)|<0, \tag{7}$$

which is an overaged Lyapunov exponent of the typical trajectory on the attractor.

Let us extract different situations related to the stability or instability of synchronized chaotic attractors on the main diagonal in the transversal direction.

(1) Even if $\lambda_2<0$, there can exist trajectories at the attractor A, for which the second Lyapunov exponent is positive. In this case we get the so-called weak stability so as the attractor A is the attractor in a weak Milnor sense [14], i.e., there exist a nonzero measure set in any neighborhood of the attractor, points of which are not attracted to A. This set is typically dense in the neighborhood of the considered attractor giving rise to the phenomenon of riddled basins.

(2) If the second Lyapunov exponent is negative for any trajectory at the attractor we get the so-called strong stability. Chaotic attractor A at the main diagonal is asymptotically stable, i.e., it attracts all trajectories from some of its neighborhood.

(3) Analogically, if $\lambda_2>0$ there can exist trajectories at the attractor A for which the averaged second Lyapunov exponent is negative. This case will be referred to as the weak instability. This phenomenon is also called on-off intermittency [29] or attractor bubbling [15].

(4) At last, if there are no such trajectories for which the second Lyapunov exponent is negative we have strong instability of the attractor on the main diagonal.

In the first two cases the considered attractor at the main diagonal can be called chaotic node, weakly attracting in case 1 and strongly attracting in case 2. Analogically, the last two cases are chaotic saddles, weak in case 3 and strong in case 4.

First, we introduce the following notation for regions of different kinds of stability of the attractors at the main diagonal. Note that if slopes l and p are fixed, stability depends only on the sum of coupling parameters $d=d_1+d_2$. Let us denote

$$D_1=\{d\in\mathbb{R}:\ \text{strong stability takes place}\},$$

$$D_2=\{d\in\mathbb{R}:\ \text{weak stability takes place}\},$$

$$D_3=\{d\in\mathbb{R}:\ \text{weak instability takes place}\},$$

$$D_4=\{d\in\mathbb{R}:\ \text{strong instability takes place}\}.$$

IV. STABILITY CONDITIONS

Stability conditions of the synchronized chaotic attractors A depend on the topological structure of chaotic attractors Γ of the one-dimensional map $f_{l,p}$. We consider three characteristic cases of attractors at the main diagonal.

A. One chaotic attractor A at the main diagonal

Let us consider $(l,p)\in\Pi$ so that the one-dimensional map $f_{l,p}$ has a single chaotic attractor Γ. In this case attractor A of the two-dimensional map $F_{l,p}$ is as follows $A=\{-1\leqslant x\leqslant 1, y=x\}$. It contains three fixed points $O^0=(0,0)$, $O^{(\pm)}=\pm(p-l)/l(p-1)$, $\pm[p-l/l(p-1)]$ which can be repelling nodes or saddles depending on d. These fixed points specify upper and lower boundaries for symbolic sequences at the attractor. These sequences are stationary and can be described as

$$PPP\ldots \qquad \text{for } O^{(\pm)}$$

and

$$LLL\ldots \qquad \text{for } O^{(0)},$$

where the following notation for symbolic sequences of the trajectories is used. We give P if $|x|>1/l$ [and consequently, $f_{l,p}(x)=p$] and L if $|x|<1/l$ [and consequently $f_{l,p}(x)=l$] is given otherwise.

Strong stability takes place if and only if the trajectories at the attractor corresponding to upper and lower boundary symbolic sequences are both saddles, i.e., they should be transversely attracting. In the case considered, it is equivalent to the following inequalities with respect to variable d:

$$|l-d|<1 \quad O^{(0)} \text{ is saddle},$$

$$|p-d|<1 \quad O^{(\pm)} \text{ is saddle},$$

which do not have common solutions for considered parameter ranges $l>1$ and $p<-1$, so in this case $D_1=\emptyset$ and strong stability is impossible.

To get strong instability, considered fixed points must be unstable nodes, i.e., $|l-d|>1$ and $|p-d|>1$. Therefore, as it can be simply obtained $D_4=(-\infty,p-1)\cup(p+1,l-1)\cup(l+1,\infty)$. Complimentary region $(p-1,p+1)\cup(l-1,l+1)$ corresponds to weak stability or instability depending on negativeness or positiveness of the second Lyapunov exponent λ_2. Therefore, weak stability (instability) takes place if and only if the parameter point (l,p) belongs to the region $(p-1,p+1)\cup(l-1,l+1)$ and, moreover,

$$|l-d||p-d|^{(\mu/1-\mu)}<1 \quad (>1), \tag{8}$$

where $\mu=\mu_{l,p}(\{|x|\geqslant 1/l\})=\mu_{l,p}([1/l,1])/2$.

In some cases (for some parameters values l and p) invariant measure $\mu_{l,p}$ can be constructed in explicit form, which allows us to find analytically the values of d at which λ_2 crosses 0 and, hence, transition from weak stability to weak instability takes place.

Example: Consider the cases of uniform probability density $\rho(x)=$const which occurs for $p=-l/(l-1)$—the graph of map $f_{l,p}(x)$ is shown in Fig. 4(a) and $p=-2l/(l-1)$ in Fig. 4(b). (Note, that in the last case invariant interval $[-1,1]$ is not an attractor of $f_{l,e}$, therefore, we can speak here on weak or strong stability in the transverse direction only.)

In both cases $\rho(x)=1/2$ for any $x\in[-1,1]$. Therefore, in the first case $p=-l(l-1)$ weak (strong) stability condition (8) is reduced to

$$|l-d|\left|\frac{l}{l-1}+d\right|^{l-1}<1 \quad (>1). \tag{9}$$

There exist four roots $d=d^{(i)}$, $i=1,4$ of the equation

$$|d-l|\left|\frac{l}{l-1}+d\right|^{l-1}=1 \tag{10}$$

such that the regions D_2 of the weak stability and D_3 of weak instability are given as (Fig. 5)

$$D_2=(d^{(1)},d^{(2)})\cup(d^{(3)},d^{(4)})$$

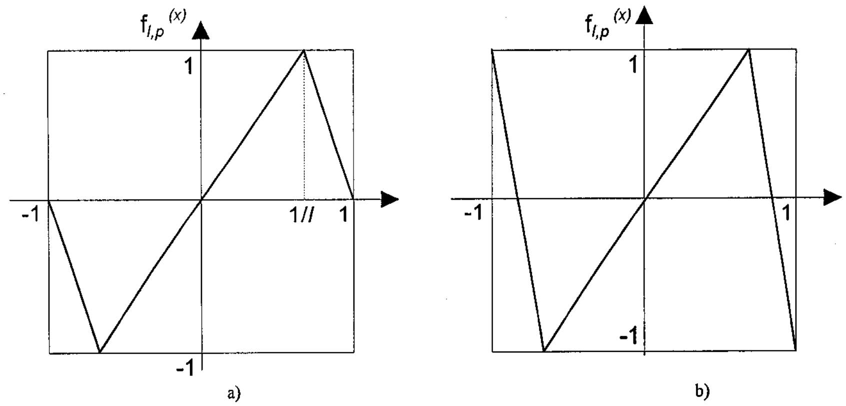

FIG. 4. Graph of the function $f_{l,p}(x)$; (a) $p=-l/(l-1)$, (b) $p=-2l/(l-1)$.

and

$$D_3=(p-1,d^{(1)})\cup(d^{(2)},p+1)\cup(l-1,d^{(3)})\cup(d^{(4)},l+1). \tag{11}$$

Remark: Parametric points $d=p$ and $d=l$ are of special interest. If the coupling parameter d has one of their values, one of the two transverse multiplicators is equal to zero. It is a case of the so-called immediate attraction. Indeed, let $d=l$ then, any initial point from the rectangle $\{|x|<1/l,|y|<1/l\}$ is attracted to the main diagonal in one iteration. Analogously, if $d=p$, any initial point from the regions $\{x<1/l, y<1/l\}$ and $\{x<-1/l,y<-1/l\}$ is attracted to the main diagonal in one iteration. Nevertheless, in both these cases only weak stability takes place, however, the basin of the attractor does not have riddled structure as it takes place when both transversal multiplicators are not equal to zero.

Generally, for any parameters $(l,p)\in\Pi$ bifurcation structure is the same as shown in Fig. 5, i.e., there exist four bifurcation values $d=d^{(i)}$, $i=1,4$ satisfying Eq. (10) and such that weak stability and weak instability regions D_2 and D_3 have form (11). The bifurcation values $d^{(i)}$, $i=1,4$ are the roots of the equation

$$|l-d||p-d|^{(\mu/1-\mu)}=1, \tag{12}$$

where $\mu=\mu_{l,p}([1/l,1])/2$.

B. Two symmetrical one-piece chaotic attractors $A^{(+)}$ and $A^{(-)}$ at the main diagonal

If parameter point (l,p) belongs to the subregion of Π_0 given by $\{l>1,-l/(l-1)<p\leqslant(1+(1+4l^2)^{1/2}/2l\}$ one-dimensional map $f_{l,p}$ has two symmetrical chaotic attractors $\Gamma^{(+)}=[1+p(l-1)/l,1]$ and $\Gamma^{(-)}=\{-1,-[1+p(l-1)/l]\}$. Consider the stability of the corresponding main diagonal attractors $A^{(+)}=\{x=y\in\Gamma^{(+)}\}$ and $A^{(-)}=\{x=y\in\Gamma^{(-)}\}$. Due to the symmetry we can restrict ourselves to the consideration of one of them, let us say $A^{(+)}$, (results for the second one would be the same). Therefore, we have come to the problem of the two coupled skew tent maps [20–23].

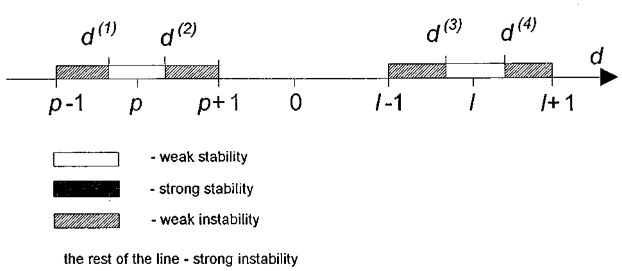

FIG. 5. Stability regions of the single chaotic attractor A at the main diagonal $x=y$.

Let us first consider strong stability and strong instability. Symbolic bounds, in this case, are given by fixed point $O^{(+)}=(l-p)/l(p-1)$ from one side and the maximal period-k cycle η_k with symbolic sequence

$$L^{k-1}PL^{k-1}P\ldots\,. \tag{13}$$

In the case of a skew tent map such a type of cycle η_k exists if and only if

$$p\leqslant-\frac{l^{k-1}-1}{(l-1)l^{k-2}},\quad k=2,3,\ldots\,.$$

Therefore, sequence (13) presents an upper symbolic boundary in the region

$$\Pi_0^{(2)}=\left\{l>1,\quad -\frac{l+1}{l}<p<\frac{1+\sqrt{1+4l^2}}{2l}\right\},$$

$$\Pi_0^{(k)}=\left\{l>1,\quad -\frac{l^k-1}{(l-1)l^{k-1}}<p<-\frac{l^{k-1}-1}{(l-1)l^{k-2}}\right\},$$

where $k=3,4\ldots$. Corresponding strong stability (instability) conditions for any region $\Pi_0^{(k)}$, $k=2,3\ldots$ are given by the system of inequalities

$$\begin{aligned}&|p-d|<1 &&(>1),\\ &|l-d|^{k-1}|p-d|<1 &&(>1),\end{aligned} \tag{14}$$

where $(l,p)\in\Pi_0^{(k)}$. In opposition to the previous case 1, strong stability region D_1 is not empty and is given as $D_1=(s_1,s_2)\ni p$. For example, in the case when $(l,p)\in\Pi_0^{(2)}$ we can find that

$$s_1=\frac{l+p-\sqrt{(l-p)^2+4}}{2}\qquad s_2=\frac{l+p-\sqrt{(l-p)^2-4}}{2}.$$

Generally, bifurcation structure is analogous to the one obtained in point 1 and is sketched in Fig. 6. $d=s^{(i)}$, $i=1,4$

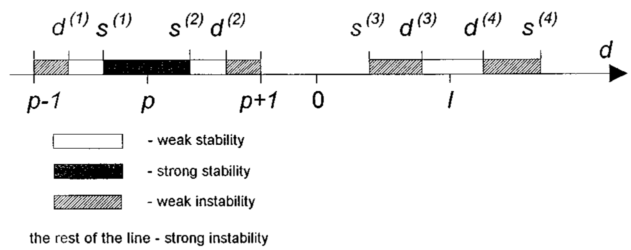

FIG. 6. Stability regions of two symmetrical one-piece chaotic attractor $A^{(+)}$ and $A^{(-)}$ at the main diagonal $x=y$.

are the roots of the equation obtained from (14) by replacing inequality to equality sign. Four bifurcation values $d=d^{(i)}$, $i=1,4$ for the transition from weak stability to weak instability are found analogically as in point 1 from the equation

$$|l-d||p-d|^{(\mu/1-\mu)}=1, \tag{15}$$

where the measure $\mu=\mu_{l,p}(\{|x|>1/l\})$.

After finding the roots we conclude that

$$D_2=(d^{(1)},s^{(1)})\cup(s^{(2)},d^{(2)})\cup(d^{(3)},d^{(4)}),$$

$$D_3=(p-1,d^{(1)})\cup(d^{(2)},p+1)\cup(s^{(3)},d^{(3)})\cup(d^{(4)},s^{(4)}),$$

and

$$D_4=(-\infty,p-1)\cup(p+1,s^{(3)})\cup(s^{(4)},\infty).$$

Example: At some parameter values invariant measure $\mu_{l,p}$ of the map $f_{l,p}$ can be easily constructed. Let us consider, $l=p/(1-p^2)$ which implies that trajectory of the extremum point $x=1/l$ put into the fixed point $O^{(+)}$ after three iterations (see Fig. 1 where the graph of $f_{l,p}$ is plotted exactly for this situation with $l=-p=\sqrt{2}$).

In this case the probability density function $\rho_{l,p}$ is two-piece constant with a break in the fixed point

$$\rho_{l,p}(x)=\begin{cases} \dfrac{l(1-p)}{2p^2(l-1)}, & x\in\left[1+\dfrac{p(l-1)}{l},\ \dfrac{p-l}{l(p-1)}\right] \\ \dfrac{l(p-1)}{2p(l\text{-}1)}, & x\in\left[\dfrac{p-l}{l(p-1)},1\right] \end{cases}$$

and condition (15) for the transition from weak stability to weak instability acquires the explicit form

$$\left|d-\frac{p}{1-p^2}\right||d-p|^{(p^2+1/p^2-1)}=1. \tag{16}$$

Equation (16) has four roots $d=d^{(i)}$, $i=1,4$ which are in the following regions:

$$d^{(1)}\in(p-1,s^{(1)}),\quad d^{(2)}\in(s^{(2)},p+1),$$

$$d^{(3)},d^{(4)}\in(s^{(3)},s^{(4)}).$$

Invariant measure $\mu_{l,p}$, can, also, be simply constructed when trajectory of the extremum point $x=1/l$ goes into the fixed point $O^{(+)}$ not after three as above but after any finite number $k>3$ iterations (we mean the trajectory, all points of which, except for $x=1$ and $x=O^{(+)}$, are to the left of $x=1/l$). Probability density function $\rho_{l,p}(x)$, in this case, is $(k-l)$-piece constant with the breaks at the points of that trajectory except from the first points of it. $\rho_{l,p}(x)$ can be simply found from this condition giving us the possibility to obtain the required measure $\mu=\mu_{l,p}(\{|x|>1/l\})$ in the explicit form.

In Figs. 7(a)–7(d) examples of weakly stable synchronized chaotic attractors $A^{(+)}$ and $A^{(-)}$ are shown. It can be easily noted [particularly at the enlargements in Figs. 7(b)–7(d)] that in the neighborhood of both attractors $A^{(+)}$ (or $A^{(-)}$), there are points which belong to the basin of the attractor at the infinity (escape to infinity) and to the basins of the other attractor $A^{(-)}$ (or $A^{(+)}$). Moreover, basins of attraction of $A^{(+)}$ and $A^{(-)}$ are riddled by the basins of these two different attractors.

In Fig. 8 we show the example of strong synchronization. It can be seen that neighborhoods of both $A^{(+)}$ and $A^{(-)}$ belong to the basins of the appropriate attractors, i.e., both $A^{(+)}$ and $A^{(-)}$ are asymptotically stable.

C. 2^m piece chaotic attractor A^m at the main diagonal

In the region $\Sigma\backslash(\Pi\cup\Pi_0)$ one-dimensional map $f_{l,p}$ has two symmetrical 2^m-piece chaotic attractors $\Gamma_m^{(\pm)}$, where m can be any positive integer. Let us consider one of them $\Gamma_m=\Gamma_m^{(+)}$, that at $x>O^{(0)}$ and study the stability of the corresponding 2^m-piece chaotic attractor A_m of the two-dimensional map $F_{l,p}$ at the main diagonal. It exists if and only if $(l,p)\in\Pi_m$, where regions Π_m are bounded by the bifurcation curves pointed out in Sec. II.

Consider a 2^m iteration of the map $f_{l,p}$, i.e., $f_{l,p}^q$, where $q=2^m$ (Fig. 9) and let $(l,p)\in\Pi_m$. In each of its 2^m invariant boxes, $f_{l,p}^q$ is a skew tent map, but having a one-piece chaotic attractor. It means, that for $f_{l,p}^q$ in each such box, we have the situation considered in point 1, moreover, slopes l_m and p_m of $f_{l,p}^q$ are as follows:

$$l_m=l^{2\alpha_{m-1}}p^{2(\alpha_{m-1}+(-1)^m)},$$

$$p_m=l^{\alpha_m}p^{\alpha_m+(-1)^m},$$

where

$$\alpha_m=\tfrac{1}{3}(2^m+(-1)^{m+1}),$$

$m=0,1,\ldots$. Therefore, the problem has been reduced to the previous case. It allows us to obtain the following stability conditions. Strong stability-instability bifurcations take place when

$$|l-d|^{\alpha_m}|p-d|^{\alpha_m+(-1)^m}=1,$$

$$|l-d|^{2(k-1)\alpha_{m-1}+\alpha_m}|p-d|^{2(k-1)[\alpha_{m-1}+(-1)^m]+\alpha_m+(-1)^m}=1, \tag{17}$$

for $\Pi_m^{(k)}=\{(l,p)\in\Pi_m\cdot(l_mp_m)\in\Pi_0^{(k)}\}$, $m=1,2\ldots$, $k=2,3\ldots$, so that the condition for the weak stability-weak instability is given by

$$|l-d|^{2\alpha_{m-1}+(\mu/1-\mu)\alpha_m}\times|p-d|^{2\{\alpha_{m-1}+(-1)^m+(\mu/1-\mu)[\alpha_m+(-1)^m]\}}=1, \tag{18}$$

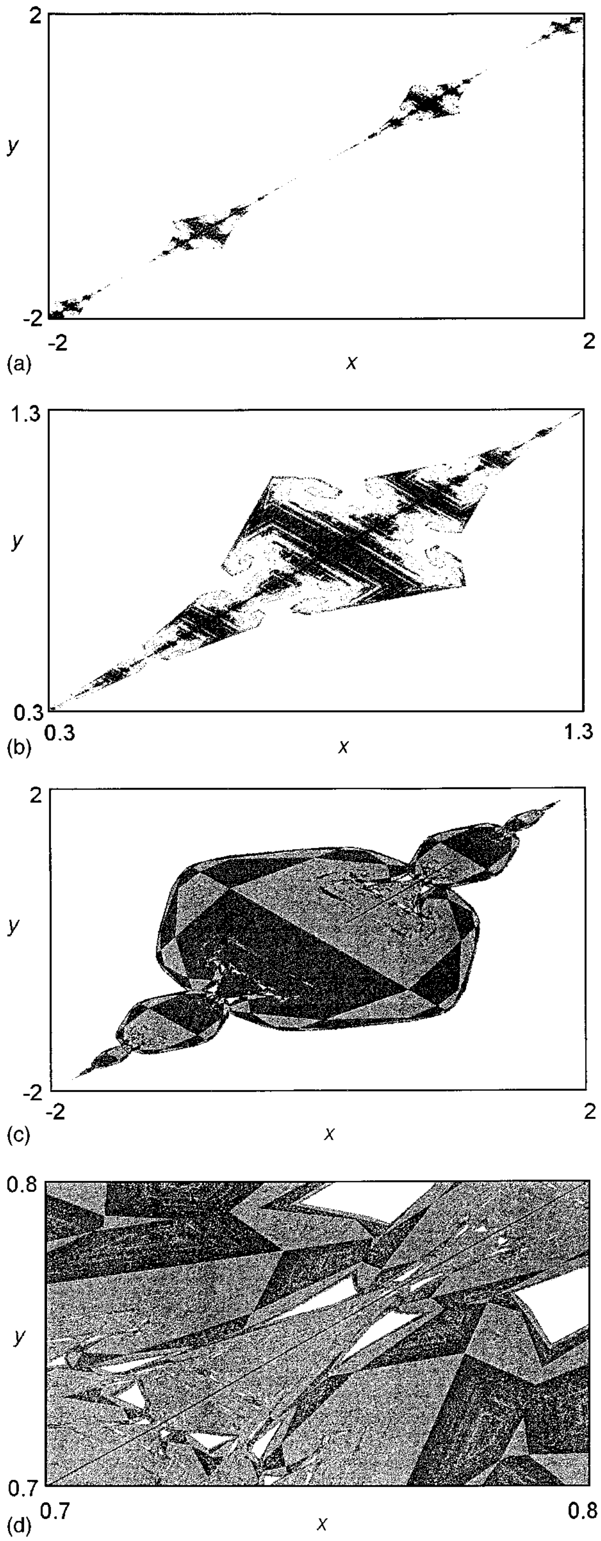

FIG. 7. Weak stability of chaotic attractors $A^{(+)}$ and $A^{(-)}$, (a) $l=-p=\sqrt{2}$, $d_1=d_2=-1$, (b) enlargement of (a), (c) $l=1.5$, $p=-2.4$, $d_1=d_2=0.65$, (d) enlargement of (c).

where

$$\mu=\mu_{l_m,p_m}\left(\left\{|x|>\frac{1}{l}\right\}\right)$$

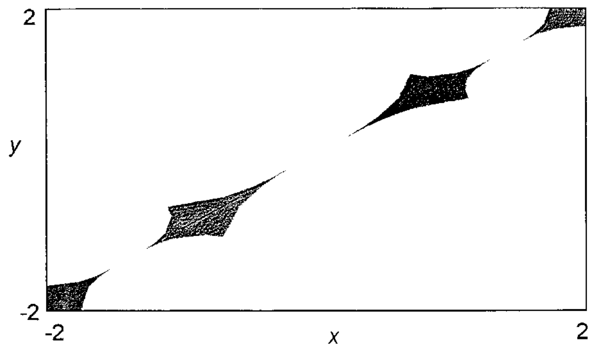

FIG. 8. Strong stability of chaotic attractors $A^{(+)}$ and $A^{(-)}$; $l=-p=\sqrt{2}$, $d_1=d_2=0.95$.

and $(l_m,p_m)\in\Pi_0$. Formulas (17) and (18) have an explicit form when the probability density function $\rho_{l,p}(x)$ can be constructed.

It can be shown that Eq. (17) has four roots $d=d^{(i)}$, $i=1,...,4$, and Eq. (18) has eight roots $d=s^{(i)}$, $i=1,...,8$ for any $m=1,2,...$ so the bifurcation structure is as shown in Fig. 10. Different stability regions are as follow:

$$D_1=(s^{(1)},s^{(3)})\cup(s^{(6)},s^{(7)}),$$

$$D_2=(d^{(1)},s^{(2)})\cup(s^{(3)},d^{(2)})\cup(d^{(3)},s^{(6)})\cup(s^{(7)},d^{(4)}),$$

$$D_3=(s^{(1)},d^{(1)})\cup(d^{(2)},s^{(4)})\cup(s^{(5)},d^{(3)})\cup(d^{(4)},s^{(8)})$$

and

$$D_4=(-\infty,s^{(1)})\cup(s^{(4)},s^{(5)})\cup(s^{(8)},\infty),$$

where roots of Eq. (18) are ordered in the following way: $s^{(i)}<s^{(i+l)}$, $i=1,7$.

In comparison with a one-piece chaotic attractor, 2^m-periodic chaotic attractors (at the main diagonal) have two d regions of strong stability.

V. CONCLUSIONS

We developed analytical conditions under which two linearly coupled one-dimensional piecewise linear endomor-

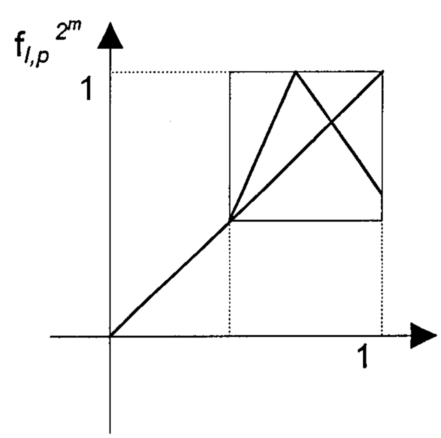

FIG. 9. Graph of the function $f_{l,p}^{2m}(x)$.

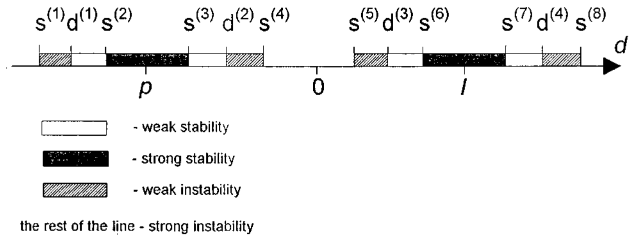

FIG. 10. Stability regions of two symmetrical two-piece chaotic attractor $A_l^{(+)}$ and $A_l^{(-)}$ at the main diagonal $x=y$.

phisms showing chaotic behavior can be synchronized. Synchronization regions for a two-dimensional map were computed based on the critical point images and probability density function of the corresponding one-dimensional map.

Our analytical conditions depend on the invariant measure of a one-dimensional map. Such measures can be easily constructed when the probability density function is known or can be simply estimated numerically. It should be mentioned here that this approach is much simpler than classical estimation of synchronization regions based on Lyapunov exponents.

Depending on the coupling parameters, the synchronized state is characterized by different types of stability. In the case of weak synchronization, the attractor of the synchronized state is not asymptotically stable, i.e., in any neighborhood of it there is the positive measure set which belongs to the basin of the other attractor. Typically, this other attractor is dense everywhere in the basin of the original one. In this case synchronization cannot be guaranteed for all slightly different initial conditions $x_0 \neq y_0$ and small perturbations to the synchronized state can permanently desynchronize both subsystems. Therefore, this type of synchronization leads to the appearance of the riddled basins and a weakly stable attractor can play the role of a ''generator'' of riddled basins.

Strong synchronization is characterized by an asymptotically stable attractor of the synchronized state $x_n = y_n$. Synchronization can be achieved for all nearby initial conditions $x_0 \neq y_0$ and when systems are synchronized they cannot be desynchronized by small perturbations. Finally, we would like to point out that the system of two linearly coupled piecewise linear endomorphisms can be easily adapted to further studies of both synchronization and riddled basins phenomena.

ACKNOWLEDGMENT

This work has been supported by the KBN (Poland) under project No. 7TO7A 039 10.

[1] H. Fuijsaka and T. Yamada, Prog. Theor. Phys. **70**, 1240 (1983).
[2] V. S. Afraimovich, N. N. Verichev, and M. I. Rabinovich, Radiophys. Quantum Electron. **29**, 795 (1986).
[3] L. Pecora and T. S. Carroll, Phys. Rev. Lett. **64**, 821 (1990).
[4] L. Pecora and T. S. Carroll, IEEE Trans. Circuits Syst. **38**, 453 (1991).
[5] V. S. Anishchenko, T. E. Vadivasova, D. E. Postnov, and M. A. Safanova, Radioeng. Electr. **36**, 338 (1991).
[6] T. Endo and L. O. Chua, Int. J. Bif. Chaos **1**, 701 (1991).
[7] M. De Sousa, A. J. Lichtenberg, and M. A. Lieberman, Phys. Rev. A **46**, 7359 (1992).
[8] Y.-C. Lai and C. Grebogi, Phys. Rev. E **47**, 2357 (1993).
[9] T. Kapitaniak, Phys. Rev. E **50**, 1642 (1994).
[10] T. Kapitaniak, L. O. Chua, and G.-Q. Zhong, Int. J. Bif. Chaos **4**, 483 (1994).
[11] K. M. Cuomo and A. V. Oppenheim, Phys. Rev. Lett. **71**, 65 (1993).
[12] U. Parlitz, L. O. Chua, L. Kocarev, K. Halle, and A. Shang, Int. J. Bif. Chaos **2**, 973 (1992).
[13] T. Kapitaniak, M. Sekieta, and M. Ogorzalek, Int. J. Bif. Chaos **6**, 211 (1996).
[14] J. Milnor, Commun. Math. Phys. **99**, 177 (1985).
[15] P. Ashwin, J. Buescu, and I. Stewart, Phys. Lett. A **193**, 126 (1994).
[16] E. Ott and J. C. Sommerer, Phys. Lett. A **188**, 39 (1994).
[17] E. Ott, J. C. Sommerer, J. C. Alexander, I. Kan, and J. A. Yorke, Physica D **76**, 384 (1994).
[18] J. C. Alexander, I. Kan, J. A. Yorke, and Z. You, Int. J. Bif. Chaos **2**, 795 (1992).
[19] J. F. Heagy, T. Carroll, and L. Pecora, Phys. Rev. Lett. **73**, 3528 (1994).
[20] T. Kapitaniak, J. Phys. A **28**, 63 (1995).
[21] V. L. Maistrenko, Yu. L. Maistrenko, and J. M. Sushko, Inst. Math. Ukr. Acad. Sci. Report No. 92.33, 1992 (unpublished).
[22] Yu. L. Maistrenko, V. L. Maistrenko, and L. O. Chua, Int. J. Bif. Chaos **3**, 1557 (1993).
[23] V. L. Maistrenko, Yu. L. Maistrenko, and J. M. Sushko, in *Chaos and Nonlinear Mechanics*, edited by T. Kapitaniak and J. Brindley (World Scientific, Singapore, 1994).
[24] D. Veitch and P. Glendinning, Physica D **44**, 149 (1990).
[25] A. S. Pikovsky and P. Grassberger, J. Phys. A **24**, 4587 (1991).
[26] L. Gardini, R. Abraham, R. J. Record, and D. Fournier-Prunaret, Int. J. Bif. Chaos **4**, 145 (1995).
[27] P. Celka, Physica D **90**, 235 (1996).
[28] H. E. Nusse and J. A. Yorke, Int. J. Bif. Chaos **5**, 189 (1995).
[29] N. Platt, E. A. Speigel, and C. Tresser, Phys. Rev. Lett. **70**, 279 (1993).